The Journal of Experimental Biology 203, 2991–3001 (2000)
Printed in Great Britain © The Company of Biologists Limited 2000
JEB2772

CHARACTERISATION OF THE H^+/PEPTIDE COTRANSPORTER OF EEL INTESTINAL BRUSH-BORDER MEMBRANES

TIZIANO VERRI[1,*], MICHELE MAFFIA[1], ANTONIO DANIELI[1], MARTINA HERGET[2], UWE WENZEL[2], HANNELORE DANIEL[2] AND CARLO STORELLI[1]

[1]*Laboratory of General Physiology, Department of Biology, University of Lecce, Strada Provinciale Lecce-Monteroni, I-73100 Lecce, Italy* and [2]*Institute of Nutritional Sciences, Physiology and Biochemistry of Nutrition, Technical University of Munich, Hochfeldweg 2, D-85350 Freising-Weihenstephan, Germany*

*e-mail: physiol@ultra5.unile.it

Accepted 8 July; published on WWW 7 September 2000

Summary

H^+/peptide cotransport in brush-border membrane vesicles (BBMVs) from eel (*Anguilla anguilla*) intestine was studied by measuring D-[^{3}H]-phenylalanyl-L-alanine uptake and by monitoring peptide-dependent intravesicular acidification using the pH-sensitive dye Acridine Orange. D-[^{3}H]-phenylalanyl-L-alanine influx was greatly stimulated by an inside-negative membrane potential and enhanced by an inwardly directed H^+ gradient. In parallel, vesicular H^+ influx was significantly increased in the presence of extravesicular D-phenylalanyl-L-alanine or a series of glycyl and L-prolyl peptides. H^+/peptide cotransport displayed saturable kinetics involving a single carrier system with apparent substrate affinities of 0.9–2.6 mmol l^{-1} depending on the particular peptide. All substrates tested competed with this system. Pre-incubation of BBMVs with dipeptides prevented diethylpyrocarbonate inhibition of transport activity, suggesting that the substrates mask histidine residues involved in the catalytic function of the transporter. Using human PepT1-specific primers, a reverse transcription–polymerase chain reaction (RT-PCR) signal was detected in eel intestine. Our results suggest that, in eel intestine, a brush-border membrane 'low-affinity'-type H^+/peptide cotransport system is present that shares kinetic features with the mammalian intestinal PepT1-type transporters.

Key words: brush-border membrane vesicle, D-phenylalanyl-L-alanine, PepT1, H^+/peptide cotransport, fish, intestine, eel, *Anguilla anguilla.*

Introduction

In higher vertebrates, intestinal absorption of di- and tripeptides arising from dietary protein digestion is mediated by electrogenic brush-border membrane transport processes. Peptide influx is coupled to an inwardly directed H^+ gradient and, in addition, is driven by the inside-negative transmembrane electrical potential (Ganapathy et al., 1994). The peptide transporters are unique among the solute transporters in that H^+ is the cotransported ion species and these carriers are able to bind and translocate an enormous number of peptides (Ganapathy et al., 1994). In addition, pharmacologically active peptide-like compounds, including β-lactam antibiotics (Kramer et al., 1992; Okano et al., 1986; Tsuji et al., 1987; Wenzel et al., 1995), angiotensin converting enzyme (ACE), inhibitors such as captopril (Hu and Amidon, 1988) and renin inhibitors (Kramer et al., 1990) serve as substrates. Recently, the molecular nature of the peptide transporters has been identified by the cloning of highly homologous cDNAs encoding transmembrane proteins that exhibit membrane-potential-dependent and pH-gradient-dependent transport of peptides and peptide-like drugs (Boll et al., 1995; Fei et al., 1994; Liang et al., 1995; Saito et al., 1995; for a review, see Daniel, 1996).

The characterisation of putative routes for fish intestinal peptide absorption is of considerable interest in aquaculture technology for both nutritional purposes and enteral delivery of peptide-like antibiotics (Michel and Alderman, 1992). H^+/glycyl-sarcosine (Gly-Sar) cotransport has been described in the brush-border membrane of absorbing cells of tilapia (*Oreochromis mossambicus*) intestine and rockfish (*Sebastes caurinus*) intestine and pyloric caeca (Thamotharan et al., 1996). Moreover, H^+/glycyl-glycine (Gly-Gly; Verri et al., 1992) and H^+/glycyl-L-proline (Gly-L-Pro; Maffia et al., 1997) cotransport has been described in eel (*Anguilla anguilla*) intestinal brush-border membranes. As in higher vertebrates, peptide uptake in teleosts occurs by carrier-mediated mechanisms and is greatly stimulated by an inside-negative transmembrane electrical potential (Maffia et al., 1997; Thamotharan et al., 1996). Furthermore, an inwardly directed transmembrane H^+ gradient has been shown to be effective in driving peptide transport either alone (Thamotharan et al.,

1996) or in cooperation with the membrane potential (Maffia et al., 1997; Thamotharan et al., 1996).

So far, a detailed kinetic analysis of intestinal brush-border membrane H^+/peptide transport activity in teleosts has not been performed, and no information is available on the molecular nature of the carrier system in fish. We therefore characterized peptide transport activity in eel intestine (i) by kinetic analysis and competition studies employing radiolabelled substrates, (ii) by H^+ influx experiments using a pH-sensitive dye and (iii) by protein modification experiments. Our studies suggest that in eel intestine a large variety of peptides share a common brush-border membrane H^+/peptide transport system similar to the mammalian intestinal PepT1-type transporter, as confirmed by reverse transcription–polymerase chain reaction (RT-PCR).

Materials and methods

European yellow eels *Anguilla anguilla*, weighing 200–250 g, were obtained from a commercial source (Ittica Ugento, Lecce, Italy) and maintained unfed for 1 week in seawater aquaria prior to use. All chemicals were reagent-grade and most were purchased from Merck (Darmstadt, Germany). Valinomycin was obtained from Sigma (St Louis, MO, USA). Custom-synthesised D-[^{3}H]-phenylalanyl-L-alanine (D-[^{3}H]-Phe-L-Ala; specific activity 333 GBq mmol^{-1}) and D-phenylalanyl-L-alanine (D-Phe-L-Ala) were obtained from Zeneca (Billingham, UK), while the fluorescent dye Acridine Orange was obtained from Eastman Kodak (Rochester, NY, USA).

Preparation of brush-border membrane vesicles

Brush-border membrane vesicles (BBMVs) were prepared from the whole intestine of yellow eels as described previously (Storelli et al., 1986). The preparation was based on the selective precipitation, in the presence of EGTA and 12 mmol l^{-1} $MgCl_2$, of all cellular components with the exception of brush-border membranes. After the final centrifugation step described by Storelli et al. (1986), BBMVs were resuspended in buffer, centrifuged at 50 000 ***g*** for 30 min and resuspended again by passing them through a 21-gauge needle. Details of buffer compositions are given in the legends to Figs 1–5 and to Table 2. Protein concentration was measured using the Bio-Rad protein assay kit, using lyophilised bovine plasma γ-globulin as a standard. Intra- and extravesicular buffers were prepared to the same ionic strength, anion concentration and osmolarity.

Uptake of D-[^{3}H]-Phe-L-Ala

Uptake of D-[^{3}H]-Phe-L-Ala was measured at 25 °C by mixing 5 µl (250 µg of protein) of BBMV suspension with 495 µl of incubation medium containing the radiolabelled peptide and variable concentrations of the unlabelled solute. Medium composition varied with the nature of the experiments and is indicated in the legends to Figs 1, 2B and 4. Solute uptake was stopped by injection of 3 ml of ice-cold stop solution containing 100 mmol l^{-1} KCl, 100 mmol l^{-1} mannitol, 20 mmol l^{-1} Hepes, adjusted to pH 7.4 with Tris. BBMVs were immediately filtered onto a Millipore filter (0.45 µm) and washed twice with an additional 3 ml of ice-cold stop solution. Filters, containing BBMVs and their associated radiolabelled solute, were placed in Beckman Ready Solv EP scintillation cocktail and counted in a Beckman LS-1801 scintillation counter. All isotope transport rates were corrected for a 'blank' obtained by adding the incubation medium and the vesicles directly to the stop solution before filtration.

Measurements of fluorescence quenching

Fluorescence signals were measured with a Perkin-Elmer LS-50B spectrofluorometer equipped with an electronic stirring system and a thermostabilised (25 °C) cuvette holder and controlled by a personal computer (PC) using Perkin-Elmer Fluorescence Data Manager software (Perkin-Elmer Ltd, Buckinghamshire, UK). Intravesicular acidification was assessed by monitoring the fluorescence quenching of the pH-sensitive dye Acridine Orange, as described previously (Maffia et al., 1997; Verri et al., 1992). Excitation and emission wavelengths were 498 and 530 nm respectively, and both slit widths were set to 5 nm. To each cuvette were added 10 µl of Acridine Orange solution (0.6 mmol l^{-1} in water), 10 µl of valinomycin solution (1 mmol l^{-1} in ethanol) and 1960 µl of a buffer with the final composition given in the legends to Figs 2A,C, 3 and 5 and to Table 2. The fluorescence intensity of this mixture was set to 90 arbitrary fluorescence units, and the reaction was started by injecting 20 µl of a vesicle suspension (250 µg of protein) into the cuvette. Fluorescence signals were recorded every 0.1 s, and the rate of fluorescence quenching was calculated from the slope through the data points collected within 5 s of the start of the reaction. Fluorescence quenching signals showed linearity as judged by regression analysis, with correlation coefficients (by the least-squares fit) of 0.98–0.99 for every experimental condition.

Kinetic analysis

Kinetic variables were determined by non-linear regression analysis, based on the Marquardt algorithm (Marquardt, 1963) using Statgraphics (STSC, Rockville, MD, USA). The kinetics of carrier-mediated D-Phe-L-Ala influx was determined by fitting experimental data to the following Michaelis–Menten-type equation with the inclusion of a non-saturable, diffusional component:

$$J = (J_{max}[S])/(K_{m,app} + [S]) + P[S], \quad (1)$$

where J is the D-Phe-L-Ala influx rate, [S] is the extravesicular D-Phe-L-Ala concentration, $K_{m,app}$ is the concentration that yielded half J_{max} and P is the permeability component of influx, calculated by linear regression through the experimental points obtained in the presence of 2 mmol l^{-1} diethylpyrocarbonate (DEP; Miyamoto et al., 1986).

Furthermore, the kinetics of carrier-mediated peptide-dependent H^+ influx was determined using a curve-fitting

procedure using the iterative non-linear regression method based on the following Michaelis–Menten-type equation:

$$\Delta F\% = (\Delta F\%_{max}[S])/(K_{m,app} + [S]), \quad (2)$$

where $\Delta F\%$ is peptide-dependent H^+ influx, $[S]$ is extravesicular peptide concentration and $K_{m,app}$ is the concentration that yielded half $\Delta F\%_{max}$.

Statistical analyses

Each experiment was repeated at least three times using membranes prepared from different animals. Within a single experiment, each data point represents 3–5 replicate measurements. Data points reported in the figures are given as means ± standard error of the mean (S.E.M.). Error bars are shown wherever they exceed the size of the symbols.

Reverse transcription–polymerase chain reaction (RT-PCR)

Total RNA was extracted from the scraped mucosa of the anterior and posterior segments of eel intestine, according to the method of Chomcyznski and Sacchi (1987). Poly(A)$^+$ RNA was isolated by chromatography on an oligo(dT)-cellulose affinity column (Sambrook et al., 1989). Poly(A)$^+$ RNA samples (1 μg) from both segments of eel intestine were subjected to RT-PCR using the GeneAmp RNA-PCR kit (PE Applied Biosystems, Foster City, CA, USA) according to the manufacturer's protocol. Briefly, reverse transcription was performed for 12 min at 42 °C in the presence of oligo(dT)$_{16}$ primer, and the resulting cDNA was subjected to PCR using human (Liang et al., 1995) PepT1-specific primers (forward primer 5′-AGCTCTTATCGCCGACTCGTG-3′, starting at nucleotide position 212; reverse primer 5′-CTTTAGCCCAGTCCAGCCAGT-3′, starting at nucleotide position 799). PCR amplification was performed for 30 cycles with 95 °C denaturation for 1 min, 55 °C annealing for 2 min and 72 °C extension for 1 min, followed by a final synthesis at 72 °C for 7 min. RT-PCR products were separated on a 1 % agarose gel and stained with ethidium bromide.

Results

D-[^{3}H]-Phe-L-Ala uptake: effects of membrane potential and pH gradient, and kinetics of peptide influx

Peptide transport was characterised in eel intestinal BBMVs by using D-Phe-L-Ala, a substrate containing a D-amino acid, which is highly resistant to hydrolysis and widely used to study peptide absorption in mammals (Amasheh et al., 1997; Lister et al., 1995).

The time course of D-Phe-L-Ala influx (0.1 mmol l^{-1}) into BBMVs preloaded with 100 mmol l^{-1} KCl, 100 mmol l^{-1} mannitol and 20 mmol l^{-1} Hepes (pH 7.4) either in the absence or in the presence of a transmembrane inside-negative electrical potential is shown in Fig. 1A. Under short-circuit conditions ($[K^+]_i$=$[K^+]_o$=100 mmol l^{-1} plus valinomycin), D-Phe-L-Ala uptake was characterised by a slow time course (open circles). In contrast, in the presence of an artificially imposed (inside-negative) membrane potential ($[K^+]_i$=100 mmol l^{-1}, $[K^+]_o$=1 mmol l^{-1} plus valinomycin), the rate of D-Phe-L-Ala influx was significantly higher (filled circles) and exhibited a transient 'overshoot' phenomenon.

To assess whether D-Phe-L-Ala transport was specifically activated by an inwardly directed H^+ gradient, uptake of 0.1 mmol l^{-1} D-Phe-L-Ala was measured in vesicles preloaded with 100 mmol l^{-1} KCl, 100 mmol l^{-1} mannitol and 20 mmol l^{-1} Hepes (pH 7.4) either in the absence or in the presence of a transmembrane H^+ gradient (pHi>pHe) under short-circuit conditions ($[K^+]_i$=$[K^+]_o$=100 mmol l^{-1} plus valinomycin). As shown in Fig. 1B, imposing an inwardly directed H^+ gradient (pHi=7.4; pHe=5.4; open circles) increased D-Phe-L-Ala uptake rate, suggesting that influx can also be enhanced by a pH gradient alone, although only modestly. These results suggest that, at the brush-border membrane of eel intestine, the electrical membrane potential (physiologically present *in vivo*) represents a highly relevant driving force of D-Phe-L-Ala transport process and that the inwardly directed H^+ gradient might be secondary to it, as found previously for Gly-L-Pro (Maffia et al., 1997). Therefore, subsequent experiments were performed in the presence of an inside-negative membrane potential only.

Uptake of D-[^{3}H]-Phe-L-Ala into eel intestinal BBMVs was linear up to 30 s (data not shown). For kinetic analysis, influx was measured for 20 s in the presence of increasing D-Phe-L-Ala concentrations (0.25–2.5 mmol l^{-1}) and in the presence of a K^+-gradient-induced inside-negative membrane potential ($[K^+]_i$=100 mmol l^{-1}, $[K^+]_o$=1 mmol l^{-1} plus valinomycin, pHi=pHe=7.4). Fig. 1C shows the total influx of D-Phe-L-Ala (filled squares) as well as the linear component obtained by treating BBMVs with 2 mmol l^{-1} diethylpyrocarbonate for 1 h (open squares). Non-linear regression analysis (see Materials and methods, equation 1) yielded a J_{max} of 1062±173 pmol mg^{-1} protein min^{-1}, a $K_{m,app}$ of 0.74±0.16 mmol l^{-1} and a permeability component (P) of 0.104±0.075 μl mg^{-1} protein min^{-1} (means ± S.E.M., N=4). These results suggest that D-Phe-L-Ala transport in eel intestinal BBMVs is a carrier-mediated process.

D-Phe-L-Ala-dependent H^+ uptake and kinetics

The effects of D-Phe-L-Ala on H^+ influx across eel intestinal BBMVs observed by monitoring Acridine Orange fluorescence quenching are shown in Fig. 2A. In the absence of a membrane potential ($[K^+]_i$=$[K^+]_o$=100 mmol l^{-1} plus valinomycin), the addition of vesicles to the cuvette in the absence (trace a) or in the presence (trace b) of 20 mmol l^{-1} D-Phe-L-Ala did not produce any significant change in Acridine Orange fluorescence quenching. However, when a transmembrane electrical potential was imposed ($[K^+]_i$=100 mmol l^{-1}, $[K^+]_o$=1 mmol l^{-1} plus valinomycin), transient fluorescence quenching due to intravesicular acidification was observed (trace c), and this was further enhanced in the presence of 20 mmol l^{-1} D-Phe-L-Ala (trace d).

The linear correlation between D-[^{3}H]-Phe-L-Ala influx and D-Phe-L-Ala-dependent H^+ influx is shown in Fig. 2B, in which net carrier-mediated D-[^{3}H]-Phe-L-Ala uptake rates are

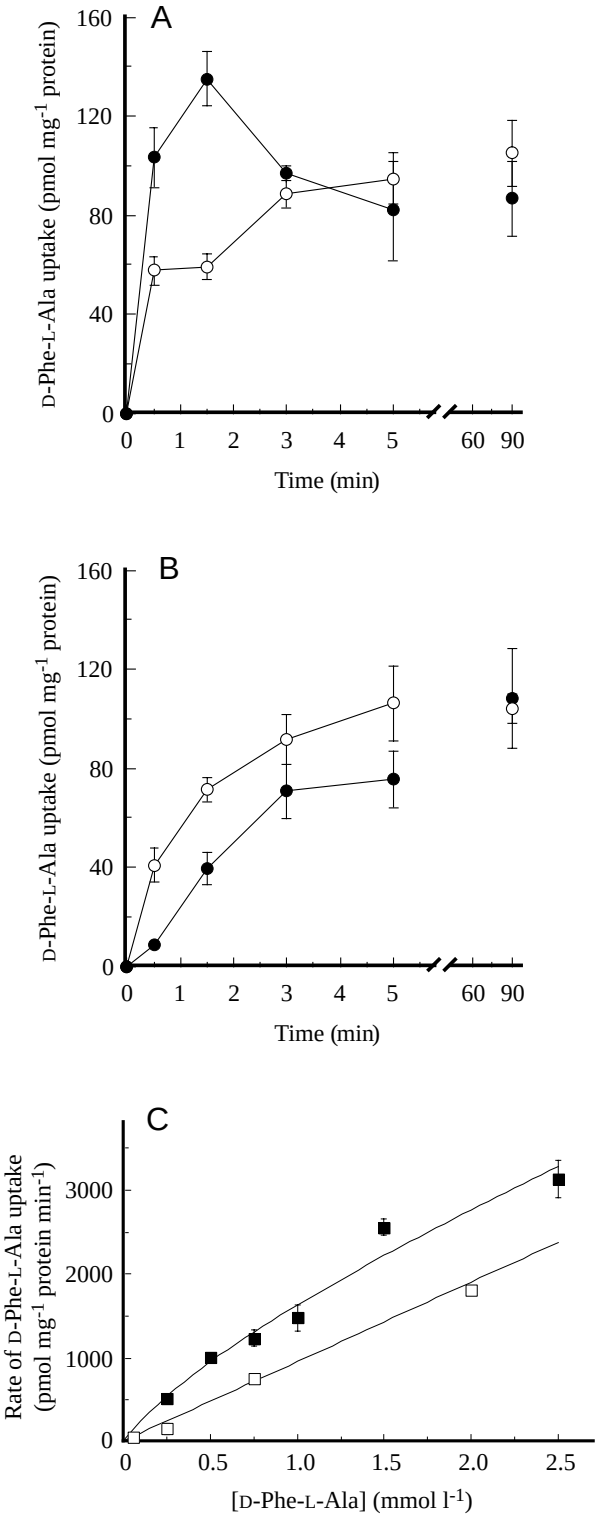

Fig. 1. (A) Time course of D-[^{3}H]-Phe-L-Ala uptake into eel intestinal brush-border membrane vesicles (BBMVs): effects of membrane potential. BBMVs were preloaded with 100 mmol l^{-1} KCl, 100 mmol l^{-1} mannitol, 20 mmol l^{-1} Hepes, adjusted to pH 7.4 with Tris. To start the experiment, 5 µl of BBMVs (250 µg of protein) was mixed with 495 µl of incubation buffer containing 100 mmol l^{-1} mannitol, 0.1 mmol l^{-1} D-Phe-L-Ala, 37 kBq of D-[^{3}H]-Phe-L-Ala, 20 mmol l^{-1} Hepes, adjusted to pH 7.4 with Tris, valinomycin (6.5 µg mg^{-1} protein) and either 100 mmol l^{-1} KCl (open circles) or 100 mmol l^{-1} choline chloride (filled circles). (B) Time course of D-[^{3}H]-Phe-L-Ala uptake into eel intestinal BBMVs: effects of a pH gradient. BBMVs (5 µl; 250 µg of protein) preloaded with 100 mmol l^{-1} KCl, 100 mmol l^{-1} mannitol, 20 mmol l^{-1} Hepes, adjusted to pH 7.4 with Tris, were mixed with 495 µl of incubation buffer containing 100 mmol l^{-1} KCl, 100 mmol l^{-1} mannitol, 0.1 mmol l^{-1} D-Phe-L-Ala, 37 kBq of D-[^{3}H]-Phe-L-Ala, valinomycin (6.5 µg mg^{-1} protein) and either 20 mmol l^{-1} Hepes, adjusted to pH 7.4 with Tris (filled circles), or 20 mmol l^{-1} Mes, adjusted to pH 5.4 with Tris (open circles). (C) Rate of uptake of D-[^{3}H]-Phe-L-Ala into eel intestinal BBMVs as a function of substrate concentration. BBMVs (5 µl; 250 µg of protein), preloaded with 100 mmol l^{-1} KCl, 100 mmol l^{-1} mannitol, 20 mmol l^{-1} Hepes, adjusted to pH 7.4 with Tris, and with (open squares) or without (filled squares) 2 mmol l^{-1} diethylpyrocarbonate, were mixed with 495 µl of incubation buffer containing 100 mmol l^{-1} choline chloride, 100 mmol l^{-1} mannitol, 0.25–2.5 mmol l^{-1} D-Phe-L-Ala, 37 kBq of D-[^{3}H]-Phe-L-Ala, valinomycin (6.5 µg mg^{-1} protein) and 20 mmol l^{-1} Hepes, adjusted to pH 7.4 with Tris. Values are means ± S.E.M., N=4.

plotted as a function of fluorescence-based D-Phe-L-Ala-dependent intravesicular acidification for D-Phe-L-Ala concentrations up to 2.5 mmol l^{-1}, in the presence of an inside-negative electrical membrane potential. Net D-Phe-L-Ala influx was calculated by subtracting the linear component obtained in the presence of 2 mmol l^{-1} diethylpyrocarbonate from total peptide uptake (as a reference, see Fig. 1C), while specific peptide-dependent H^+ influx was determined by subtracting the fluorescence quenching in the absence of peptide from that obtained in the presence of peptide (as a reference, see Fig. 2A, traces c and d). That intravesicular acidification under these conditions is solely dependent on peptide influx is documented by the good correlation between the fluorescence quench rates and the corresponding D-[^{3}H]-Phe-L-Ala influx rates (y-axis intercept 0.92; slope 7.34; r^2=0.93 in Fig. 2B). The intercept y-value of approximately 1 pmol 0.25 mg^{-1} protein s^{-1} probably represents the lack of change in intracellular pH because of the internal buffering capacity of the vesicles. Only when peptide/H^+ influx is increased at higher substrate concentrations are the corresponding changes in intravesicular pH detectable.

The kinetics of D-Phe-L-Ala transport was therefore determined by monitoring peptide-dependent H^+ influx in the presence of increasing peptide concentrations. H^+ influx was a hyperbolic function of D-Phe-L-Ala concentration (Fig. 2C). The corresponding Woolf–Augustinsson–Hofstee plot (Segel, 1975) is also shown (see inset to Fig. 2C), and this suggests that D-Phe-L-Ala-dependent H^+ influx occurs by a single carrier-mediated process. In addition, the kinetics of dipeptide transport was also determined for a variety of dipeptides by monitoring peptide-dependent H^+ influx. As for D-Phe-L-Ala, Gly-Gly, Gly-L-Pro, Gly-Sar, glycyl-L-asparagine (Gly-L-Asn), glycyl-L-alanine (Gly-L-Ala) and L-prolyl-glycine (L-Pro-Gly) caused H^+ influx with a hyperbolic dependence on peptide concentration. For all peptides tested, the kinetic variables were calculated by non-linear regression

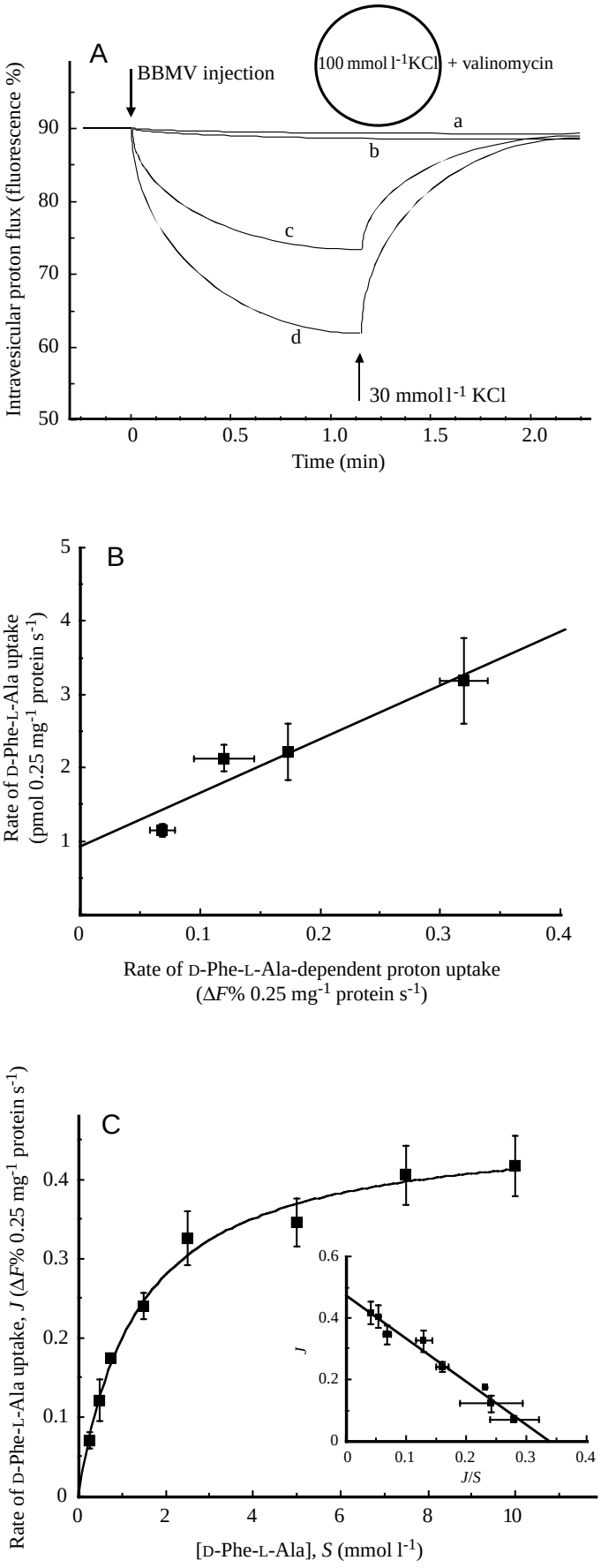

Fig. 2. (A) Peptide-dependent Acridine Orange fluorescence quenching in eel intestinal brush-border membrane vesicles (BBMVs). BBMVs were prepared in a buffer containing 100 mmol l^{-1} KCl, 100 mmol l^{-1} mannitol, 2 mmol l^{-1} Hepes, adjusted to pH 7.4 with Tris. To start the experiment, 20 µl of BBMVs (250 µg of protein) was injected into 1980 µl of cuvette buffer containing 3 µmol l^{-1} Acridine Orange, 5 µmol l^{-1} valinomycin, 0.5 % ethanol, 100 mmol l^{-1} mannitol, 2 mmol l^{-1} Hepes, adjusted to pH 7.4 with Tris, and 100 mmol l^{-1} KCl (trace a), 100 mmol l^{-1} KCl and 20 mmol l^{-1} D-Phe-L-Ala (trace b), 100 mmol l^{-1} choline chloride (trace c) or 100 mmol l^{-1} choline chloride and 20 mmol l^{-1} D-Phe-L-Ala (trace d). When present, peptides replaced mannitol iso-osmotically. To obtain faster re-equilibration of the transient transmembrane H^+ asymmetry, 20 µl of 3 mol l^{-1} KCl solution was added into the cuvette at the time indicated. (B) Comparison between net D-[^{3}H]-Phe-L-Ala influx rates and net D-Phe-L-Ala-dependent H^+ influx rates in eel intestinal BBMVs. Net D-[^{3}H]-Phe-L-Ala and net D-Phe-L-Ala-dependent H^+ influx rates were measured at peptide concentrations of 0.25, 0.5, 0.75 and 2.5 mmol l^{-1} and compared by plotting, for each peptide concentration, peptide influx rate *versus* peptide-dependent H^+ influx rate. To measure net carrier-mediated D-[^{3}H]-Phe-L-Ala influx, BBMVs (5 µl; 250 µg of protein), preloaded with 100 mmol l^{-1} KCl, 100 mmol l^{-1} mannitol, 2 mmol l^{-1} Hepes, adjusted to pH 7.4 with Tris, and with or without 2 mmol l^{-1} diethylpyrocarbonate, were mixed with 495 µl of incubation buffer containing 100 mmol l^{-1} choline chloride, 100 mmol l^{-1} mannitol, 37 kBq of D-[^{3}H]-Phe-L-Ala, valinomycin (6.5 µg mg^{-1} protein), 2 mmol l^{-1} Hepes, adjusted to pH 7.4 with Tris, and 0.25, 0.5, 0.75 or 2.5 mmol l^{-1} D-Phe-L-Ala. Net D-Phe-L-Ala influx was calculated by subtracting values obtained in the presence of 2 mmol l^{-1} diethylpyrocarbonate from those obtained in its absence (as a reference, see Fig. 1C). To measure net D-Phe-L-Ala-dependent H^+ influx, BBMVs (20 µl; 250 µg of protein), preloaded with 100 mmol l^{-1} KCl, 100 mmol l^{-1} mannitol, 2 mmol l^{-1} Hepes, adjusted to pH 7.4 with Tris, were injected into 1980 µl of incubation buffer containing 3 µmol l^{-1} Acridine Orange, 5 µmol l^{-1} valinomycin, 0.5 % ethanol, 100 mmol l^{-1} choline chloride, 100 mmol l^{-1} mannitol, 2 mmol l^{-1} Hepes, adjusted to pH 7.4 with Tris, and 0, 0.25, 0.5, 0.75 or 2.5 mmol l^{-1} D-Phe-L-Ala, iso-osmotically compensated by decreasing mannitol concentrations. Net peptide-dependent H^+ influx was determined by subtracting values of fluorescence quenching (ΔF%) obtained in the absence of D-Phe-L-Ala (as a reference, see Fig. 2A, traces c) from values obtained in the presence of increasing peptide concentrations (as a reference, see Fig. 2A, trace d). Measurements of influx rates were performed on the same BBMV preparation and are normalized by time (s) and the amount of protein (250 µg). Values are means ± S.E.M., N=4. (C) Dependence of the initial rate of H^+ influx on increasing extravesicular D-Phe-L-Ala concentrations. BBMVs (20 µl; 250 µg of protein), prepared in a buffer containing 100 mmol l^{-1} KCl, 100 mmol l^{-1} mannitol, 2 mmol l^{-1} Hepes, adjusted to pH 7.4 with Tris, were injected into 1980 µl of an incubation buffer containing 3 µmol l^{-1} Acridine Orange, 5 µmol l^{-1} valinomycin, 0.5 % ethanol, 100 mmol l^{-1} choline chloride, 100 mmol l^{-1} mannitol, 2 mmol l^{-1} Hepes, adjusted to pH 7.4 with Tris, and 0.25–10 mmol l^{-1} D-Phe-L-Ala, iso-osmotically compensated by decreasing mannitol concentrations. Net peptide-dependent H^+ fluxes are reported. The inset gives experimental data for the initial rates of D-Phe-L-Ala-dependent H^+ fluxes reported in the main body of the figure transformed according to the method of Woolf–Augustinsson–Hofstee. Values are means ± S.E.M., N=4.

Table 1. *Kinetic variables of H^+/peptide cotransport by eel intestinal brush-border membrane vesicles*

Substrate	$K_{m,app}$ (mmol l^{-1})	$\Delta F\%_{max}$ ($\Delta F\%$ 0.25 mg^{-1} protein s^{-1})	Number of experiments
D-Phe-L-Ala	1.19±0.52	0.46±0.06	3
Gly-L-Pro	1.04±0.31	0.27±0.02	5
Gly-Gly	1.81±0.49	0.54±0.04	7
Gly-L-Ala	0.97±0.42	0.73±0.07	3
Gly-L-Asn	2.59±0.73	0.47±0.04	3
Gly-Sar	1.75±0.47	0.31±0.16	4
L-Pro-Gly	0.87±0.36	0.06±0.02	3

Kinetic variables were obtained by monitoring peptide-dependent H^+ influx using the pH-sensitive dye Acridine Orange in the presence of increasing concentrations of single peptides up to 10 mmol l^{-1}.

$\Delta F\%_{max}$, maximal peptide-dependent H^+ influx; $K_{m,app}$, concentration yielding half $\Delta F\%_{max}$.

Values are expressed as means ± S.E.M.

analysis (see Materials and methods, equation 2); they are given in Table 1. Linear relationships in Woolf–Augustinsson–Hofstee plots similar to that reported in the inset to Fig. 2C were obtained for these other tested peptides (data not shown).

Substrate specificity and peptide interaction at a common transport system

Specific peptide-dependent H^+ influx was measured at saturating concentrations of several peptides (Fig. 3). Substrate-mediated H^+ fluxes were observed with neutral di- and tripeptides as well as with the negatively charged glycyl-L-aspartate (Gly-L-Asp). L-prolyl peptides, e.g. L-Pro-Gly and L-prolyl-L-alanine (L-Pro-L-Ala), also accelerated H^+ influx, although less effectively than D-Phe-L-Ala or the glycyl peptides containing either two or three amino acid residues. In addition, Gly-L-Pro, glycyl-L-hydroxyproline (Gly-L-Hyp) and glycyl-L-prolyl-L-alanine (Gly-L-Pro-L-Ala) exhibited a tendency to lower maximal velocities with respect to D-Phe-L-Ala and the other glycyl peptides.

To assess whether different peptides interact at a common transport site, the inhibitory effects of Gly-L-Pro on D-[^{3}H]-Phe-L-Ala transport were first examined. Influx of D-[^{3}H]-Phe-L-Ala was measured at concentrations of 0.25–5 mmol l^{-1} in the absence and presence of 1 and 4 mmol l^{-1} Gly-L-Pro under the same experimental conditions as in Fig. 1C. Net carrier-mediated D-[^{3}H]-Phe-L-Ala transport was obtained after subtracting the non-saturable D-[^{3}H]-Phe-L-Ala influx measured in the presence of 2 mmol l^{-1} diethylpyrocarbonate from the total D-[^{3}H]-Phe-L-Ala influx determined in the absence of diethylpyrocarbonate. The corresponding Woolf–Augustinsson–Hofstee plot for the carrier-mediated flux is shown in Fig. 4. Linear regression analysis for data obtained in the absence of Gly-L-Pro (filled squares) or in the presence of 1 mmol l^{-1} (filled triangles) and 4 mmol l^{-1} Gly-L-Pro (open squares) shows a common *y*-axis intercept, establishing that inhibition of D-Phe-L-Ala transport by Gly-L-Pro is competitive in nature. The apparent K_i of Gly-L-Pro, obtained by replotting the slopes ($-K_{m,app}$) of the individual Woolf–Augustinsson–Hofstee curves against the corresponding inhibitor concentrations (Segel, 1975), was 1.29±0.06 mmol l^{-1} (inset to Fig. 4).

To analyse further peptide competition at the transporter binding site, pairs of peptides (either Gly-Gly or D-Phe-L-Ala plus a second different peptide) were added at saturating concentrations (20 mmol l^{-1}) to the extravesicular medium, and the corresponding changes in H^+ flux rates were measured (Table 2). Substrate-mediated H^+ flux rates caused by pairs of peptides were found to depend on the maximal H^+ flux that could be induced by each individual peptide (Table 2). When a second peptide was applied to a peptide solution that caused only small H^+ flux rates (low apparent maximal velocity), a much higher maximal H^+ influx was observed. In the case of peptides that themselves caused high H^+ flux rates, the addition of a second substrate never induced

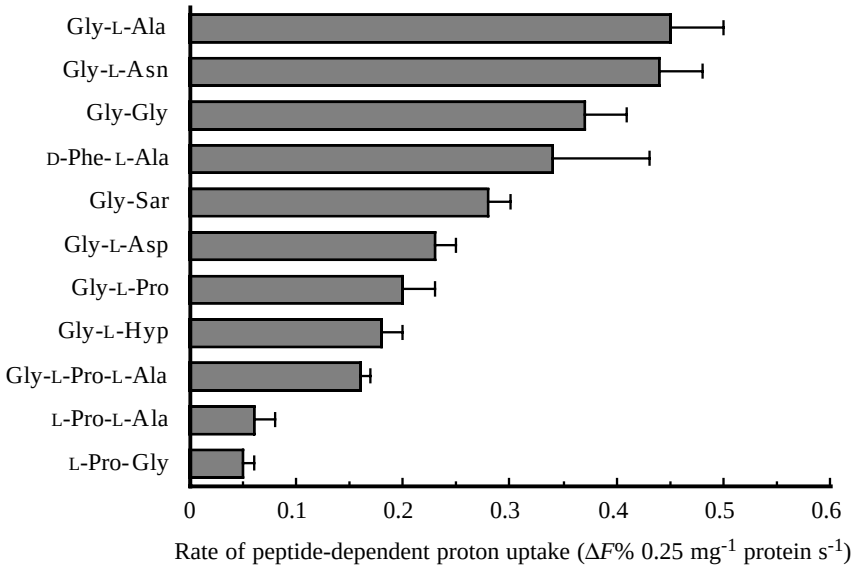

Fig. 3. Effects of exogenous di- and tripeptides on H^+ influx rate. The rate of peptide-dependent H^+ influx was estimated by subtracting H^+ uptake (fluorescence quenching, $\Delta F\%$) in the absence from that in the presence of 20 mmol l^{-1} of each individual peptide under the same experimental conditions reported in Fig. 2A (compare trace d with trace c). The results shown in the figure are means + S.E.M. of experimental data obtained from seven different membrane preparations. D-Phe-L-Ala, D-phenylalanyl-L-alanine; Gly-Gly, glycyl-glycine; Gly-L-Ala, glycyl-L-alanine; Gly-L-Asn, glycyl-L-asparagine; Gly-L-Asp, glycyl-L-aspartate; Gly-L-Hyp, glycyl-L-hydroxyproline; Gly-L-Pro, glycyl-L-proline; Gly-L-Pro-L-Ala, glycyl-L-prolyl-L-alanine; Gly-Sar, glycyl-sarcosine; L-Pro-Gly, L-prolyl-glycine; L-Pro-L-Ala, L-prolyl-L-alanine.

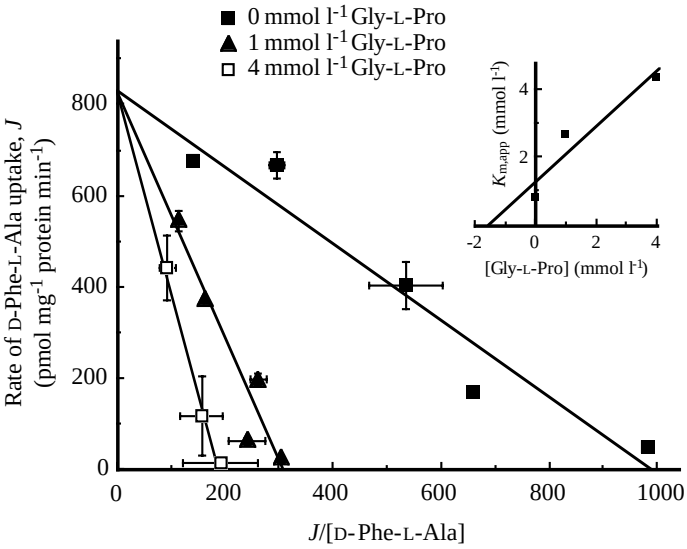

Fig. 4. Inhibition of D-[^{3}H]-Phe-L-Ala uptake by Gly-L-Pro. Brush-border membrane vesicles (BBMVs) (5 µl; 250 µg of protein), preloaded with 100 mmol l^{-1} KCl, 100 mmol l^{-1} mannitol, 20 mmol l^{-1} Hepes, adjusted to pH 7.4 with Tris, with or without 2 mmol l^{-1} diethylpyrocarbonate, were mixed with incubation buffer (495 µl) containing 100 mmol l^{-1} choline chloride, 100 mmol l^{-1} mannitol, 0.25–5 mmol l^{-1} D-Phe-L-Ala, 37 kBq of D-[^{3}H]-Phe-L-Ala, valinomycin (6.5 µg mg^{-1} protein), 20 mmol l^{-1} Hepes, adjusted to pH 7.4 with Tris, plus 0 mmol l^{-1} (filled squares), 1 mmol l^{-1} (filled triangles) or 4 mmol l^{-1} (open squares) Gly-L-Pro. For each experimental condition, values obtained in the presence of 2 mmol l^{-1} diethylpyrocarbonate were subtracted from total uptake and net carrier-mediated D-Phe-L-Ala transport shown according to a Woolf–Augustinsson–Hofstee plot. Uptake was measured using a 20 s incubation. In the inset, the slope ($-K_{m,app}$) of each Woolf–Augustinsson–Hofstee curve has been plotted against the corresponding inhibitor Gly-L-Pro concentration at which it was obtained to calculate the negative inhibitory constant ($-K_i$) for Gly-L-Pro. J indicates D-Phe-L-Ala uptake and is expressed in pmol mg^{-1} protein min^{-1}; D-Phe-L-Ala concentration is expressed in mmol l^{-1}. Values are means ± S.E.M., N=4.

Table 2. *Competition for peptide-dependent H^+ influx in eel intestinal brush-border membrane vesicles by the simultaneous presence of pairs of peptides*

Single peptides (20 mmol l^{-1})		Pairs of peptides (20 mmol l^{-1} each)		
Peptide-dependent H^+ flux (ΔF% 0.25 mg^{-1} protein s^{-1})		Peptide-dependent H^+ flux (ΔF% 0.25 mg^{-1} protein s^{-1})		Competition (%)
	A			
Gly-Gly	0.31±0.04			
	B		C	C/(A+B)100
Gly-L-Pro	0.17±0.01	Gly-Gly+Gly-L-Pro	0.20±0.02	41.6
Gly-Sar	0.28±0.01	Gly-Gly+Gly-Sar	0.29±0.03	49.1
Gly-L-Hyp	0.22±0.02	Gly-Gly+Gly-L-Hyp	0.23±0.04	43.4
L-Pro-Gly	0.14±0.02	Gly-Gly+L-Pro-Gly	0.28±0.02	62.2
L-Pro-L-Ala	0.13±0.02	Gly-Gly+L-Pro-L-Ala	0.29±0.02	65.9
	D			
D-Phe-L-Ala	0.36±0.04			
	E		F	F/(D+E)100
Gly-L-Ala	0.56±0.03	D-Phe-L-Ala+Gly-L-Ala	0.45±0.06	48.9
Gly-Gly	0.48±0.01	D-Phe-L-Ala+Gly-Gly	0.45±0.03	53.6
Gly-L-Pro	0.19±0.03	D-Phe-L-Ala+Gly-L-Pro	0.21±0.07	38.2
Gly-L-Hyp	0.20±0.02	D-Phe-L-Ala+Gly-L-Hyp	0.24±0.01	42.9
Gly-L-Asp	0.21±0.06	D-Phe-L-Ala+Gly-L-Asp	0.19±0.02	33.3
L-Pro-L-Ala	0.15±0.02	D-Phe-L-Ala+L-Pro-L-Ala	0.25±0.03	49.0
L-Pro-Gly	0.16±0.05	D-Phe-L-Ala+L-Pro-Gly	0.32±0.04	61.5

20 µl of brush-border membrane vesicles, preloaded with 100 mmol l^{-1} KCl, 100 mmol l^{-1} mannitol, 2 mmol l^{-1} Hepes, adjusted to pH 7.4 with Tris, were mixed with 1980 µl of incubation buffer containing either 100 mmol l^{-1} choline chloride, 80 mmol l^{-1} mannitol, 20 mmol l^{-1} Gly-Gly (or 20 mmol l^{-1} D-Phe-L-Ala), 2 mmol l^{-1} Hepes, adjusted to pH 7.4 with Tris (control), or 100 mmol l^{-1} choline chloride, 60 mmol l^{-1} mannitol, 20 mmol l^{-1} Gly-Gly (or 20 mmol l^{-1} D-Phe-L-Ala), 2 mmol l^{-1} Hepes, adjusted to pH 7.4 with Tris, plus 20 mmol l^{-1} of a second peptide.

Two separate experiments are reported.

ΔF%, peptide dependent H^+ influx.

Values are means ± S.E.M. of 6 experiments.

a further increase in H^+ influx. With all combinations of peptides, maximal intravesicular acidification rates represented the mean value of that caused by the corresponding individual substrates. These findings strongly suggested that all the substrates utilised the same route and that maximal H^+ flux rates were dependent on the maximal velocity of the transporter with a given substrate. That the maximal H^+ flux rates obtained were indeed a function of the transporter velocity and not caused by limitations of the test system was proved by measuring H^+ influx induced by the protonophore carbonylcyanid-3-chlorphenylhydrazone (CCCP; 1 mmol l^{-1}). Here, the initial rate of membrane-potential-induced intravesicular acidification was several times higher than the initial H^+ flux rates observed in the presence of peptides (data not shown).

Prevention of diethylpyrocarbonate inhibition by peptides

Diethylpyrocarbonate has been shown to inhibit mammalian peptide transporters by interacting with histidine residues (Fei et al., 1997; Miyamoto et al., 1986; Terada et al., 1996). In Fig. 5, we show that treatment of eel intestinal BBMVs with 2 mmol l^{-1} diethylpyrocarbonate also inhibits approximately 80–90 % of peptide-dependent H^+ influx. However, addition of an excess of peptides to the medium prior to incubation of the BBMVs with diethylpyrocarbonate completely protected peptide-dependent H^+ influx from inhibition by diethylpyrocarbonate. In particular, we observed that pre-incubation with Gly-L-Pro protected Gly-L-Pro-dependent H^+ influx (Fig. 5A) and that pre-incubation with Gly-Sar protected Gly-Sar-dependent H^+ influx (Fig. 5B). Gly-Sar protected Gly-L-Pro-dependent H^+ flux (Fig. 5C) and Gly-L-Pro protected Gly-Gly-dependent H^+ flux (Fig. 5D). These findings again suggest that peptides interact at the same transporter binding site, and that the diethylpyrocarbonate-reactive histidyl residues in the eel peptide transporter are located at or near important catalytic site(s).

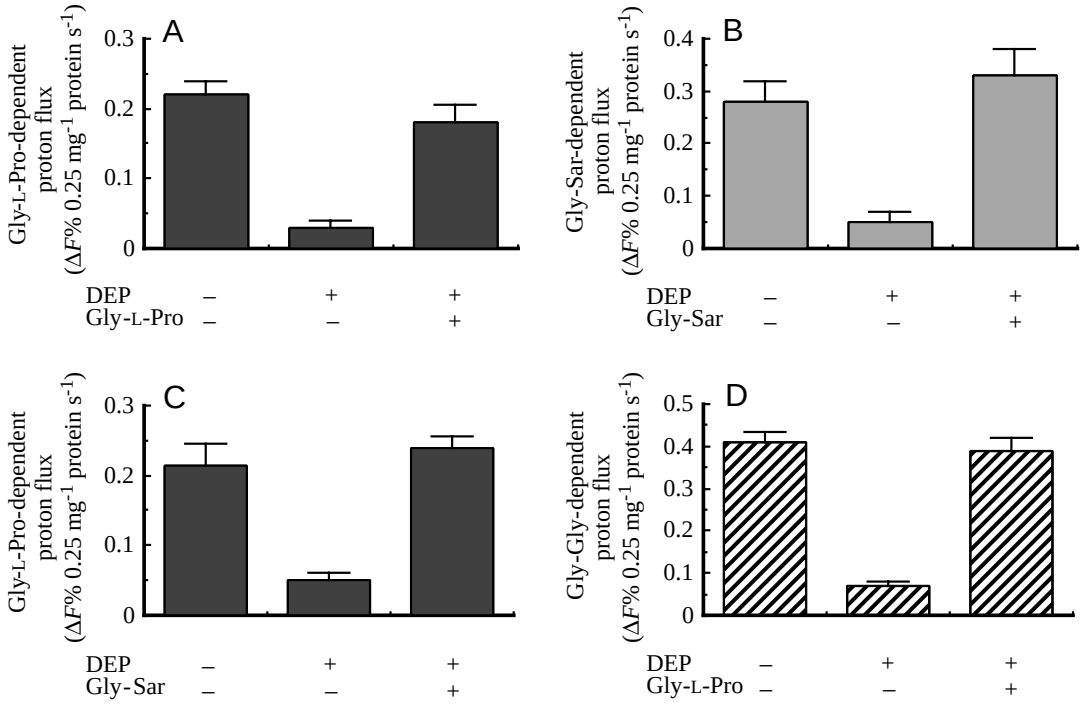

Fig. 5. Prevention of diethylpyrocarbonate inhibition by extravesicular incubation with peptides. Brush-border membrane vesicles (BBMVs) were incubated for 40 min at 18 °C in buffer containing either 280 mmol l^{-1} mannitol, 20 mmol l^{-1} K_2HPO_4/KH_2PO_4, pH 6.4, or 260 mmol l^{-1} mannitol, 20 mmol l^{-1} K_2HPO_4/KH_2PO_4, pH 6.4, and 20 mmol l^{-1} of peptide (Gly-L-Pro) (A,D) or Gly-Sar (B,C). After this incubation, BBMVs in the above buffers were further incubated for 1 h at 18 °C either in the presence (from a 100 mmol l^{-1} ethanol stock solution) or in the absence (ethanol only) of 2 mmol l^{-1} diethylpyrocarbonate (DEP). In any case, the final ethanol concentration did not exceed 1 %. Then, to eliminate the excess diethylpyrocarbonate, which affects the Acridine Orange fluorescence signal, diethylpyrocarbonate-treated and untreated BBMVs were diluted in 35 ml of buffer containing 100 mmol l^{-1} mannitol, 100 mmol l^{-1} KCl, 2 mmol l^{-1} Hepes, adjusted to pH 7.4 with Tris, and centrifuged at 50 000 ***g*** for 30 min. This washing procedure was repeated twice. To start the experiment, BBMVs (20 µl; 250 µg of protein) loaded with 100 mmol l^{-1} mannitol, 100 mmol l^{-1} KCl and 2 mmol l^{-1} Hepes, adjusted to pH 7.4 with Tris, were injected into 1980 µl of cuvette buffer containing 3 µmol l^{-1} Acridine Orange, 5 µmol l^{-1} valinomycin, 0.5 % ethanol and either 100 mmol l^{-1} choline chloride, 100 mmol l^{-1} mannitol and 2 mmol l^{-1} Hepes, adjusted to pH 7.4 with Tris (control), or 100 mmol l^{-1} choline chloride, 80 mmol l^{-1} mannitol and 2 mmol l^{-1} Hepes, adjusted to pH 7.4 with Tris, plus 20 mmol l^{-1} Gly-L-Pro (A,C) or Gly-Sar (B) or Gly-Gly (D). Net peptide-dependent H^+ fluxes were obtained by subtracting H^+ flux in the absence of peptide (control) from the total H^+ flux in the presence of each peptide and are expressed as ΔF% 0.25 mg^{-1} protein s^{-1}, where ΔF% is fluorescence quenching. Values are means + S.E.M., N=4.

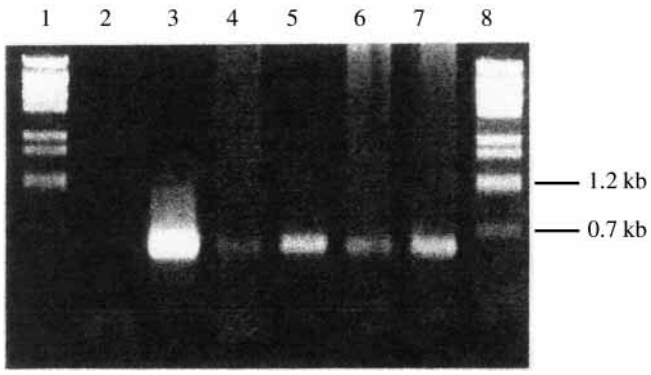

Fig. 6. Expression of PepT1-related mRNA in eel intestine by RT-PCR. mRNA isolated from the anterior and the posterior segments of eel intestine was subjected to reverse transcription (RT), and the resulting cDNA was amplified by polymerase chain reaction (PCR) using human PepT1-specific primers (see Materials and methods for details). Lanes 1 and 8, λBstE II digest size marker (New England Biolabs, Schwalbach, Germany); lane 2, negative control (H_2O); lane 3, positive control (human PepT1 cDNA, 5 ng); lanes 4 and 6, eel intestine, anterior segment (two different first-strand syntheses); lanes 5 and 7, eel intestine, posterior segment (two different first-strand syntheses). kb, kilobase.

Detection of a RT-PCR product in eel intestine by human PepT1-specific primers

Using human-specific primers designed on the basis of the human small intestinal PepT1 cDNA sequence (Liang et al., 1995; for further details, see Materials and methods), PepT1-related RT-PCR products of approximately 550 base pairs (bp) could be amplified from mRNA isolated from both the anterior and the posterior segments of eel intestine (Fig. 6). Nucleotide sequence showed 54 % similarity to human PepT1 and encoded for an amino acid sequence with 56 % similarity to human PepT1 (data not shown). These data strongly support the hypothesis that a PepT1-related mRNA product is present in the mRNA pool isolated from eel intestine, suggesting that a PepT1-related protein may be responsible for peptide transport across the brush-border membrane of eel intestinal absorbing cells.

Discussion

Recent studies suggest that peptide transport across the apical membrane of intestinal cells of a variety of teleost fish is mediated by saturable transport systems similar to those found in higher vertebrates (Maffia et al., 1997; Thamotharan et al., 1996; Verri et al., 1992). Although some of the basic characteristics of peptide transport in fish have been determined, there has been no detailed analysis of the kinetics of transport of different substrates and of the question of whether more than one peptide transporter phenotype is involved in uptake. With the focus on the eel intestine, we provide evidence that a large variety of di- and tripeptides are transported across the brush-border membrane by a saturable transport system (Fig. 1–4; Table 1, 2). All peptides induced the movement of H^+ into the intravesicular space (Figs 2, 3; Table 1) in support of the presence of a peptide/H^+ cotransporter. Peptide influx into eel intestinal BBMVs was found to be dependent on membrane potential and to a lesser extent on the H^+ gradient (Fig. 1); analogously, peptide-dependent H^+ movement showed a strict dependence on membrane potential (Fig. 2A). Moreover, intravesicular acidification rates correlated, in the case of D-Phe-L-Ala, with dipeptide influx rates, indicating a fixed coupling stochiometry for H^+/peptide cotransport over a large concentration range (Fig. 2B).

Taken together, these findings suggest that eel intestine possesses an apical peptide transporter that operates electrogenically by coupling substrate transport to the movement of protons down an electrochemical proton gradient.

On the basis of proton influx measurements, we show that all peptides caused intravesicular acidification following Michaelis–Menten-type kinetics with apparent affinity constants ranging from 0.87 to 2.59 mmol l^{-1} (Table 1). These results are comparable with those previously reported in tilapia (*Oreochromis mossambicus*) (Thamotharan et al., 1996) and eel (*Anguilla anguilla*) (Maffia et al., 1997) intestinal BBMVs. Moreover, they parallel data obtained for apical membrane peptide transport in Caco-2 cells (Thwaites et al., 1993; Brandsch et al., 1994) for the renal 'low-affinity' transport system (Daniel et al., 1991) and for the mammalian intestinal peptide transporter PepT1 (Fei et al., 1994). However, in eel intestinal BBMVs, we found a low K_m value (0.87 mmol l^{-1}) for L-Pro-Gly, which contrasts with the high K_i value (22 mmol l^{-1}) recently reported for the same substrate in CaCo-2 cells (Brandsch et al., 1999), although the V_{max}/K_m ratio of L-Pro-Gly suggests a lower transport efficiency for this substrate compared with the other peptides tested.

Maximal proton influx rates varied considerably (see Fig. 3; Table 1). The lowest H^+ flux rates were recorded for dipeptides containing an L-proline residue, whereas peptides containing L-alanine, glycine, D-phenylalanine or L-aspartate residues showed proton influx rates up to three times higher. This suggests that prolyl peptides are either transported by a lower H^+/substrate stoichiometry or that their maximal transport rate and, therefore, proton influx rate is lower while the flux coupling ratio is the same as for the other peptides. Studies on the cloned mammalian peptide transporters have consistently shown that zwitterionic dipeptides are generally transported by a 1:1 flux coupling ratio (Amasheh et al., 1997). It seems reasonable, therefore, to assume that the zwitterionic dipeptides L-Pro-L-Ala, L-Pro-Gly and Gly-L-Pro also have the same flux coupling ratio as other peptides. The observed lower maximal proton transport rate in the presence of the prolyl peptides may therefore indeed represent the lower transporter velocity. This could be a consequence of the particular conformational constraints in these substrates. The imino acid function in the prolyl peptides causes the peptide bond to deviate from planarity and, because of these steric constraints, the prolyl peptides may hinder the transporter from operating at its maximal velocity. In addition, peptides possessing C-terminal

prolyl residues are also known for their tendency to form *cis*-conformers of the peptide bond. As demonstrated very recently, such dipeptides with a *cis* peptide bond are not transported by the mammalian PepT1 (Brandsch et al., 1998). Prolyl peptides therefore represent a separate class of substrates that show lower transport rates compared with almost all the other di- or tripeptides consisting of L-α-amino acids.

That the eel peptide transport system also transports charged substrates is shown by the intravesicular acidification caused by glycyl-L-aspartate, which carries a net negative charge at pH 7.4 (Fig. 3). The rate of proton influx induced by Gly-L-Asp is similar to that caused by neutral dipeptides such as Gly-Sar, suggesting that the flux coupling ratio is also not different from that of zwitterionic substrates. Studies with PepT1 expressed in oocytes revealed that acidic dipeptides, including Gly-L-Asp, have a similar transport rate to zwitterionic substrates and have a comparable, if not identical, flux coupling ratio for H^+/peptide flux (Amasheh et al., 1997).

There is some controversy about the presence of multiple peptide transporters in the intestine of fish (Thamotharan et al., 1996). Our studies provide clear evidence for the presence of just one system, at least within the 0.1–10 mmol l^{-1} range, although they do not exclude the possibility that other peptide transporters might operate at lower and/or higher concentration ranges. Kinetic analysis of both dipeptide influx and peptide-mediated proton influx revealed a single saturable system (Figs 2C, 4). Moreover, all the peptides employed appeared to interact at the same substrate-binding site of the transporter. This is supported (i) by the competitive nature of the interaction observed between Gly-Pro and D-Phe-Ala influx (Fig. 4), (ii) by the characteristics of peptide-mediated proton influx when using a large variety of combinations of peptides (Table 2) and (iii) by the ability of different substrates to protect the diethylpyrocarbonate-sensitive sites in the transporter from modification by this histidyl-reactive agent (Fig. 5).

The observation that peptides protect transport activity from diethylpyrocarbonate inhibition (Fig. 5) strongly suggests that diethylpyrocarbonate-reactive residues are also found in or close to the substrate-binding site of the eel transporter. In higher vertebrates, specific diethylpyrocarbonate-reactive residues, e.g. histidyl residues 57 and 121 (Fei et al., 1997; Terada et al., 1996), have been shown to be crucial for transporter function. These histidyl residues are suggested to be involved in H^+ binding and translocation. Whereas mutations of histidine 57 in both rat and human PepT1 transporters completely blocked transport, mutations of histidine 121 appeared to abolish transport activity only in the human PepT1, but not in the rat PepT1. Although we have no information about the transporter protein, our studies reveal that active site histidyl residues in the eel transporter are essential for function, as judged by loss of proton transport capability after diethylpyrocarbonate treatment and in substrate protection studies.

In addition, by using human PepT1-specific primers, a RT-PCR product was detected (Fig. 6), suggesting that a PepT1-like H^+/peptide cotransporter mRNA may be present in the mRNA pool extracted from eel intestinal mucosa. Signals associated with both the anterior and the posterior parts of the intestine indicate that the putative PepT1-like peptide transporter may be expressed along the whole intestine of the fish, a finding that differs from that for the small intestinal distribution of PepT1 in mammals (see, for instance, Fei et al., 1994). However, further studies are required to address this question fully.

In summary, the results reported in this study suggest the presence of a H^+/peptide carrier system in eel intestinal BBMVs. Its kinetic, functional and molecular features relate it to the mammalian intestinal brush-border membrane PepT1-type transporters. A PepT1-like carrier with a high transport capacity could play a major role in amino acid absorption since carnivorous fish possess a relatively short intestine (only a few centimeters long) compared with that of omnivorous or herbivorous vertebrate species, in which the gut length may be several times the body length. This characterization of the peptide transporter of eel intestinal brush-border membranes provides new information about a route for the delivery of growth-limiting amino acids, thus representing a tool in the formulation of new diets for aquaculture. Moreover, the capability of PepT1-type carriers to transport β-lactam antibiotics, such as amino-cephalosporins, could provide the opportunity for treatment of bacterial diseases in fish *via* the oral route. Besides these practical applications, cloning of the intestinal PepT1-like transport system of a fish would allow important insights into the molecular structure and function of vertebrate peptide transporters.

This investigation was supported by the Italian Ministry of Agriculture, Food and Forestry (Fourth Plan on Fisheries and Aquaculture in Marine and Brackish Waters) and by the 'Programma Nazionale Ricerche in Antartide'. T.V. is the recipient of a post-doctoral fellowship from the Italian Ministry for Agricultural Politics (ex Ministry of Agriculture, Food and Forestry). We are grateful to Alfredo Giuseppe Pede for his skilful technical assistance.

References

Amasheh, S., Wenzel, U., Boll, M., Dorn, D., Weber, W.-M., Clauss, W. and Daniel, H. (1997). Transport of charged dipeptides by the intestinal H^+/peptide symporter PepT1 expressed in *Xenopus laevis* oocytes. *J. Membr. Biol.* **155**, 247–256.

Boll, M., Markovich, D., Weber, W. M., Korte, H., Daniel, H. and Murer, H. (1995). Expression cloning of a cDNA from rabbit small intestine related to proton-coupled transport of peptides, β-lactam antibiotics and ACE-inhibitors. *Pflügers Arch.* **429**, 146–149.

Brandsch, M., Knütter, I., Thunecke, F., Hartrodt, B., Born, I., Börner, V., Hirche, F., Fischer, G. and Neubert, K. (1999). Decisive structural determinants for the interaction of proline derivatives with the intestinal H^+/peptide symporter. *Eur. J. Biochem.* **266**, 502–508.

Brandsch, M., Miyamoto, Y., Ganapathy, V. and Leibach, F. H. (1994). Expression and protein kinase C-dependent regulation of peptide/H^+ cotransport system in the Caco-2 human colon carcinoma cell line. *Biochem. J.* **299**, 253–260.

Brandsch, M., Thunecke, F., Küllertz, G., Schutkowski, M., Fischer, G. and Neubert, K. (1998). Evidence for the absolute conformational specificity of the intestinal H^+/peptide symporter, PEPT1. *J. Biol. Chem.* **273**, 3861–3864.

Chomcyznski, P. and Sacchi, N. (1987). Single-step method of RNA isolation by guanidinium thiocyanate–phenol–chloroform extraction. *Analyt. Biochem.* **162**, 156–159.

Daniel, H. (1996). Function and molecular structure of brush border membrane peptide/H^+ symporters. *J. Membr. Biol.* **154**, 197–203.

Daniel, H., Morse, E. L. and Adibi, S. A. (1991). The high and low affinity transport systems for dipeptides in kidney brush border membrane respond differently to alterations in pH gradient and membrane potential. *J. Biol. Chem.* **266**, 19917–19924.

Fei, Y. J., Kanai, Y., Nussberger, S., Ganapathy, V., Leibach, F. H., Romero, M. F., Singh, S. K., Boron, W. F. and Hediger, M. A. (1994). Expression cloning of a mammalian proton-coupled oligopeptide transporter. *Nature* **368**, 563–566.

Fei, Y. J., Liu, W., Prasad, P. D., Kekuda, R., Oblak, T. G., Ganapathy, V. and Leibach, F. H. (1997). Identification of the hystidyl residue obligatory for the catalytic activity of the human H^+/peptide cotransporters PepT1 and PepT2. *Biochemistry* **36**, 452–460.

Ganapathy, V., Brandsch, M. and Leibach, F. H. (1994). Intestinal transport of amino acids and peptides. In *Physiology of the Gastrointestinal Tract* (ed. L. R. Johnson), pp. 1773–1794. New York: Raven Press.

Hu, M. and Amidon, G. L. (1988). Passive- and carrier-mediated intestinal absorption components of captopril. *J. Pharm. Sci.* **77**, 1007–1011.

Kramer, W., Girbig, F., Gutjahr, U., Kleemann, H. W., Leipe, I., Urbach, H. and Wagner, A. (1990). Interaction of renin inhibitors with the intestinal uptake system for oligopeptides and β-lactam antibiotics. *Biochim. Biophys. Acta* **1027**, 25–30.

Kramer, W., Girbig, F., Gutjahr, U., Kowalewski, S., Adam, F. and Schiebler, W. (1992). Intestinal absorption of β-lactam antibiotics and oligopeptides. *Eur. J. Biochem.* **204**, 923–930.

Liang, R., Fei, Y. J., Prasad, P. D., Ramamoorthy, S., Han, H., Yang-Feng, T. L., Hediger, M. A., Ganapathy, V. and Leibach, F. H. (1995). Human intestinal H^+/peptide cotransporter. *J. Biol. Chem.* **270**, 6456–6463.

Lister, N., Sykes, A. P., Bailey, P. D., Boyd, C. A. R. and Bronk, J. R. (1995). Dipeptide transport and hydrolysis in isolated loops of rat small intestine: effect of stereo-specificity. *J. Physiol., Lond.* **484**, 173–182.

Maffia, M., Verri, T., Danieli, A., Thamotharan, M., Pastore, M., Ahearn, G. A. and Storelli, C. (1997). H^+/glycyl-L-proline cotransport in brush border membrane vesicles of eel (*Anguilla anguilla*) intestine. *Am. J. Physiol.* **272**, R217–R225.

Marquardt, D. W. (1963). An algorithm for least squares estimation of non linear parameters. *J. Soc. Indust. Appl. Math.* **11**, 431–441.

Michel, C. and Alderman, D. J. (1992). *Chemotherapy in Aquaculture: from Theory to Reality*. Paris: Office International des Epizooties (OIE).

Miyamoto, Y., Ganapathy, V. and Leibach, F. H. (1986). Identification of histidyl and thiol groups at the active site of rabbit renal dipeptide transporter. *J. Biol. Chem.* **261**, 16133–16140.

Okano, T., Inui, K., Maegawa, H., Takano, M. and Hori, R. (1986). H^+ coupled uphill transport of aminocephalosporins *via* the dipeptide transport system in rabbit intestinal brush-border membranes. *J. Biol. Chem.* **261**, 14130–14134.

Saito, H., Okuda, M., Terada, T., Sasaki, S. and Inui, K. I. (1995). Cloning and characterization of a rat H^+/peptide cotransporter mediating absorption of β-lactam antibiotics in the intestine and kidney. *J. Pharmac. Exp. Ther.* **275**, 1631–1637.

Sambrook, J., Fritsch, E. F. and Maniatis, T. (1989). *Molecular Cloning. A Laboratory Manual.* Second edition. Cold Spring Harbor, NY: Cold Spring Harbor Laboratory.

Segel, I. H. (1975). *Enzyme Kinetics. Behaviour and Analysis of Rapid Equilibrium and Steady-State Enzyme Systems*, pp. 100–159. New York: J. Wiley & Sons.

Storelli, C., Vilella, S. and Cassano, G. (1986). Na-dependent D-glucose and L-alanine transport in eel intestinal brush border membrane vesicles. *Am. J. Physiol.* **251**, R463–R469.

Terada, T., Saito, H., Mukai, M. and Inui, K. (1996). Identification of the histidine residues involved in substrate recognition by a rat H^+/peptide cotransporter, PepT1. *FEBS Lett.* **394**, 196–200.

Thamotharan, M., Gomme, J., Zonno, V., Maffia, M., Storelli, C. and Ahearn, G. A. (1996). Electrogenic, proton-coupled, intestinal dipeptide transport in herbivorous and carnivorous teleosts. *Am. J. Physiol.* **270**, R939–R947.

Thwaites, D. T., Brown, C. D. A., Hirst, B. H. and Simmons, N. L. (1993). H^+-coupled dipeptide (glycylsarcosine) transport across apical and basal borders of human intestinal Caco-2 cell monolayers display distinctive characteristics. *Biochim. Biophys. Acta* **1151**, 237–245.

Tsuji, A., Tamai, I., Hirooka, H. and Terasaki, T. (1987). β-lactam antibiotics and transport *via* the dipeptide carrier system across the intestinal brush-border membrane. *Biochem. Pharmac.* **36**, 565–567.

Verri, T., Maffia, M. and Storelli, C. (1992). H^+-glycyl-glycine cotransport in eel intestinal brush-border membrane vesicles: studies with the pH-sensitive dye Acridine orange. *Biochim. Biophys. Acta* **1110**, 123–126.

Wenzel, U., Thwaites, D. T. and Daniel, H. (1995). Stereoselective uptake of β-lactam antibiotics by the intestinal peptide transporter. *Br. J. Pharmac.* **116**, 3021–3027.